NUMERICAL SCHWARZ-CHRISTOFFEL METHODS IN ELECTROMAGNETIC COMPATIBILITY ANALYSIS*

A.P.J. van Deursen[(1)] **and S. Kapora**[(2)]

[(1)] ***Department of Electrical Engineering, Eindhoven University of Technology***
POB 513, 5600 MB Eindhoven, The Netherlands, e-mail: a.p.j.v.deursen@tue.nl

[(2)] ***United Technical Solutions B.V., POB 6285, 5600 HG Eindhoven, The Netherlands.***

ABSTRACT

Numerical Schwarz-Christoffel methods for simply connected regions provide accurate values for the inductive coupling on printed circuit boards and between the boards and the environment. Cabinet panels can be included by the methods for doubly connected regions. A differential pair of tracks shows unexpected increase of coupling in nearly closed cabinets.

INTRODUCTION

In the past few years advanced numerical programs to solve the parameter problem in Schwarz-Christoffel (SC) transformations have become available. We applied this method to two-dimensional configurations with interest in the field of electromagnetic compatibility (EMC). By virtue of the near-to-exact numerical SC approach, setups with very small couplings have been modelled accurately. Most setups discussed can be described by elements of Fig. 1. First, omit the cabinet and consider the flat groundplane and tracks extending in the direction perpendicular to the complex plane. The Joukowski transform maps the ground plane onto the unit-circle, and readily delivers the inductive coupling M' (in H/m) between tracks, and between a track and the environment [1]. Secondly, omit the groundplane and keep the ⊔-shape, which now represents a metal cable conduit. The corresponding transforms first map the ⊔-shape onto the rectangle between $\pm(K + iK')$ by the Jacobi Zeta function, and secondly map the rectangle onto the unit-circle again [2]. The exponential decrease of inductive coupling for cables deeper in the conduit is discussed in [3].

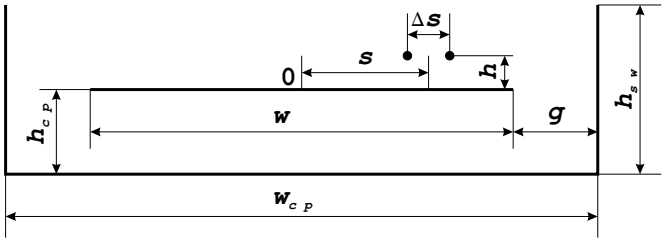

Figure 1: Cross-section of a PCB inside a U-shaped cabinet panel, with a pair of track indicated.

The numerical SC toolbox [4] can deal with more complicated structures, such as a non-contacting ⊓-cover symmetrically placed on top of the ⊔-conduit. When the finite metal thickness was included, the large number of corners necessitated a numerical approach to obtain the parameters. The inductive coupling for a cable inside the conduit and an external current or an external magnetic field agreed with measurements [5].

The combination of a printed circuit board (PCB) groundplane and cabinet panel (Fig. 1) requires a SC-description by doubly connected regions. The main part of the paper will present some of the results obtained by this approach, and whenever possible compare them with those by Method of Moments (MoM). A full account is given in [6].

Figure 1 shows the cross-section of a typical configuration. The PCB consists of a continuous groundplane (GP) of width $w = 100$ mm. A single thin wire represents a track at $h = 1$ mm above or below the GP and at variable distance s from the middle of the GP. In case of a differential pair, both tracks are at identical height. Their separation is $\Delta s = 1$ mm and s is measured with respect to the mid-position between the wires. Such a PCB is symmetrically placed inside the U-shaped metal cabinet panel (CP) of width $w_{cp} = w + 2g$ with sidewalls of the height $h_{sw} = 20$ mm. The GP is at the height $h_{cp} = 10$ mm above the CP.

*Portions reprinted from [6], with permission of IEEE. All figures ©IEEE.

SC TRANSFORM

The Schwarz-Cristoffel integral for the mapping function reads [7]:

$$f(w) = C \int^{w} \frac{\prod_{k=1}^{m} \left[\theta\left(\frac{w'}{\mu w_{0k}}\right)\right]^{\alpha_{0k}-1} \prod_{k=1}^{n} \left[\theta\left(\frac{\mu w'}{w_{1k}}\right)\right]^{\alpha_{1k}-1}}{\left[w'\ \theta\left(\frac{w_\infty}{w'}\right)\theta\left(\frac{w^*_\infty}{w'}\right)\right]^2} dw' \quad \text{with} \quad \theta(w) = \prod_{d=1,3,5,\cdots} (1-\mu^d w)(1-\mu^d/w). \tag{1}$$

The θ-function are described in [8, Eqs 17.5-4]. The function $z = f(w)$ maps the annulus $\mu < |w| < 1$ in the complex w-plane onto the exterior of two disjoint polygons described by sets of vertices z_{0k} with $k = 1, \cdots, m$ and z_{1k} with $k = 1, \cdots, n$ in the complex z-plane. The subscripts indicate whether the prevertices $w_{\{0,1\}k}$ are on the outer (0) or the inner (1) circle. The exponents in (1) are related to the outer angles $\pi\alpha_{\{0,1\}k}$ of the polygons and obey the relations $\sum \alpha_{0k} = m+2$ and $\sum \alpha_{1k} = n+2$. The denominator in (1) ensures that w_∞ is mapped onto infinity in the z-plane. It is convenient to chose w_∞ on the real axis $\mu < w_\infty < 1$; $w^*_\infty = \mu^2/w_\infty$ is the image of w_∞ with respect to the inner circle. This choice uniquely determines the arguments $\phi_{\{0,1\}k}$ of the prevertices $w_{\{0,1\}k}$. The $\phi_{\{0,1\}k}$ and the parameters μ, w_∞ and C follow from a non-linear fitting procedure [9]. The $m+n+4$ fitting object functions are the directions and lengths $z_{11} - z_{1n}$, $z_{01} - z_{0m}$ and $z_{1n} - z_{0m}$, and $m+n-2$ lengths of the remaining polygon sides. We let the inner circle correspond to the ground plane ($n = 2$), and the outer circle to the cabinet panel ($m = 6$). On a present day laptop computer the fit required about one second to converge with the desired maximum deviation of the object functions set at 10^{-12}.

$\mu = 0.650825362804$
$w_\infty = 0.9045881776270778$
$C = -0.199 \times 10^{-11} + i * 0.2767398576959381$

k	$z_0(k)$	$\alpha_0(k)$	$\phi_0(k)$
1	-0.55	0.5	1.0087535282594999
2	0.55	0.5	5.2744317788897028
3	0.55+0.2i	2.0	6.0345068421694652
4	0.55	1.5	6.2112250037584751
5	-0.55	1.5	6.3551456106005810
6	-0.55+0.2i	2.0	0.2486784650094369
k	$z_1(k)$	$\alpha_1(k)$	$\phi_1(k)$
1	0.5+0.1i	2.0	5.5345240005527776
2	-0.5+0.1i	2.0	0.7486613066124166

Table 1: Parameters for the typical GP-CP example with $z_{\{0,1\}k}$ in units of 100 mm.

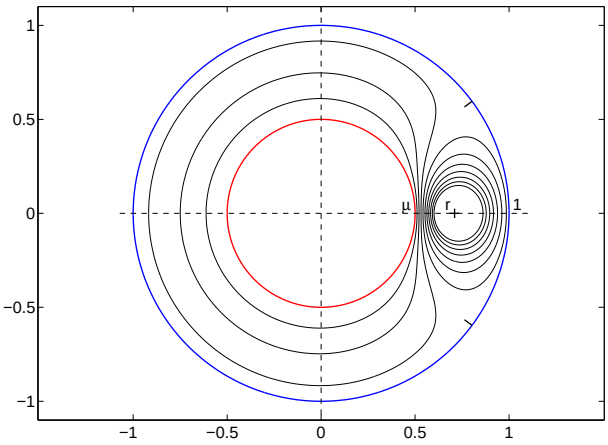

Figure 2: Magnetic field lines due to a line current at $r = 0.71$ (+) between the cylinders $|w| = 1$ and $|w| = \mu = 0.5$.

The parameters in Table 1 have been obtained for the typical PCB example with $z_{\{0,1\}k}$ in units of 100 mm. The results are accurate at least to the first 6 digits. These parameters need to be determined only once per GP-CP configuration. The inductive coupling follows from the complex potential function of a wire carrying a current I between the two perfectly conducting cylinders. Assume the wire on the real axis at r, $\mu < r < 1$, with a logarithmic potential $(-iI/2\pi) \times log(w-r)$ at point w. Both cylinder generate an infinite series of mirror images, and all images sum up to

$$W(w) = -\frac{iI}{2\pi} \log \frac{\theta(\mu w/r)}{\theta(\mu w r)}. \tag{2}$$

The imaginary part V of W is the magnetic flux function. Inspection of the real part of (2) shows that the current returns through the outer circle. If one adds the potential

$$W_1(w) = \frac{iI}{2\pi} \log(w) \tag{3}$$

to $W(w)$, the current returns through the inner circle. Examples of magnetic field lines for this case are shown in Fig. 2; the magnetic field and current density are zero at the markers on the outer circle. If W_1 is multiplied by $\log(r)/\log(\mu)$, the return current distributes over both circles and the magnetic flux between them is zero. This occurs when the conductors represented by the circles are interconnected at their ends.

INDUCTIVE COUPLING

Consider track(s) on top of the CP, and a fixed gap $g = 5$ mm (Fig. 1). The mutual inductance M' between track and the environment has been calculated from the magnetic flux between the track and GP due to a current I through the GP with a return $-I$ at infinity or $r = w_\infty$ in (2): $M' = (\mu_0/I)\,[V(w_t) - V(\mu)]$,where w_t is the image of the track position z_t.

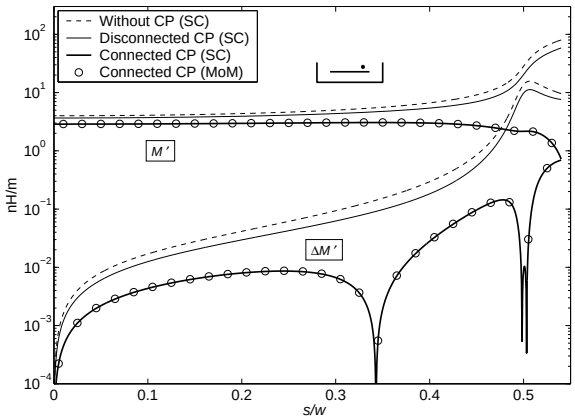

Figure 3: M' and $|\Delta M'|$ for tracks above the GP.

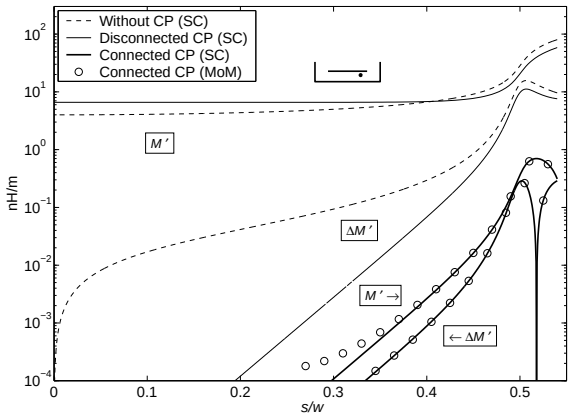

Figure 4: M' and $|\Delta M'|$ for tracks under the GP.

Figure 3 shows the M'-results for: a) no cabinet present (dashed lines), b) with cabinet but not connected to the GP (thin solid line), and c) with interconnected GP and CP (thick solid line). Even an electrically floating CP (case b) decreases the coupling, be it by about a factor of 2 at most. When the CP and GP are properly connected at both ends in the third dimension (case c), the current is shared by the GP and the CP such that no magnetic flux passes between them. For a track approaching the PCB edge, M' now decreases compared to case a) and b); at the GP edge ($s/w = 0.5$) the reduction is a factor of 10. The reduction is mainly caused by the sidewalls. Fig. 3 also shows $\Delta M'$, the difference in coupling for a balanced pair of tracks, which is also strongly reduced by the CP. From a first order Taylor expansion of $M'(s)$ one concludes that $\Delta M' \simeq \Delta s \times \partial M'/\partial s$. The deep minima at $s/w = 0$ and 0.35 and near $s/w = 0.5$ stem from a zero derivative of $M'(s)$. The MoM data – shown only for the connected CP case – agree very well with the SC values.

Figure 4 shows the results for the track(s) below the GP for the same three cases. When the GP and CP are connected (case c), the wires are positioned between two plates. The potential deeper between the plates varies $\propto e^{\pi s/h_{cp}}$. Both M' and $\Delta M'$ follow this exponential behavior down to very small s. The ratio $\Delta M'/M'$ becomes constant, equal to $\pi \Delta s/h_{cp} \simeq 0.3$, independent on the track height for equal $h_{1,2}$. For a single track and disconnected CP (case b) the changes with respect to case a) are minor: a reduction of about a factor of 2 for a track near the edge, and remarkably enough an increase by the same factor when the track is near the GP center. On the other hand $\Delta M'$ decreases substantially in accordance with the levelling-off of M' for $s/w < 0.4$. In fact, $\Delta M'$ varies again $\propto e^{\pi s/h_{cp}}$ for small s. Due to the inherent finite numerical accuracy, the MoM data start to deviate for very small M'. Doubling of the number of elements from 1000 to 2000 reduces the difference between MoM and SC from about a factor of 4.5 to 1.3 for the lowest M' shown at $s/w = 0.27$.

The inductive coupling strongly depends on the shape of the cabinet. We started from the 110 mm wide cabinet base, and extended the CP by adding metal of length ℓ at each side to a total of $110 + 2\ell$ mm. We then compared three situations: a) flat horizontal extensions of the base, b) vertical sidewalls of height ℓ, and c) the same sidewalls up to $h_{sw} = 20$ mm, but now folded inwards starting at the height h_{sw} so that fins of length $\ell - h_{sw}$ are formed; see the thick lines of the insets in Fig. 5. The single track is near the edge at $s/w = 0.497$ and either on top of or below the GP. Because the disconnected CP has nearly no effect, only the results for the connected CP are shown. The added flat metal (a) is least effective, as M' decreases only slowly with ℓ. In situation b) about an order of magnitude reduction is obtained at $\ell = 20$ mm, equal to h_{sw} of the typical setup. At larger ℓ, the sidewalls form two parallel plates and the exponential decrease $\propto e^{-\pi \ell/w_{cp}}$ sets in. Situation c) confirms the intuitive guess that it is better to fold the sidewalls and bend them inwards over the PCB. The steeper descent is proportional to $e^{-\pi \ell/(h_{sw} - h_{cp})}$, because the track is now in a slit formed by the GP and a fin, acting as parallel plates at the distance of $h_{sw} - h_{cp} = 10$ mm.

This does not necessarily imply that $\Delta M'$ is also improved, because of the increased derivative $\partial M'/\partial s$. As

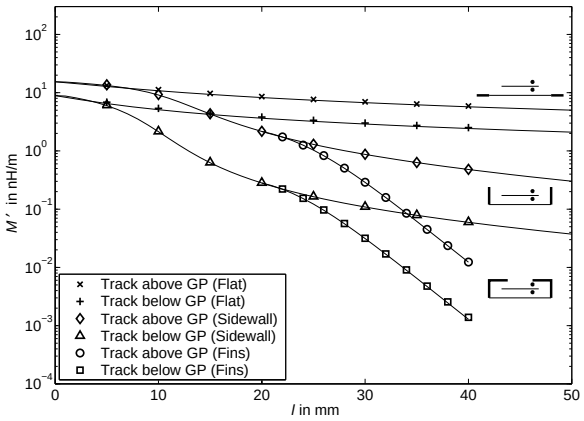

Figure 5: M' versus added metal length ℓ. The markers are MoM data.

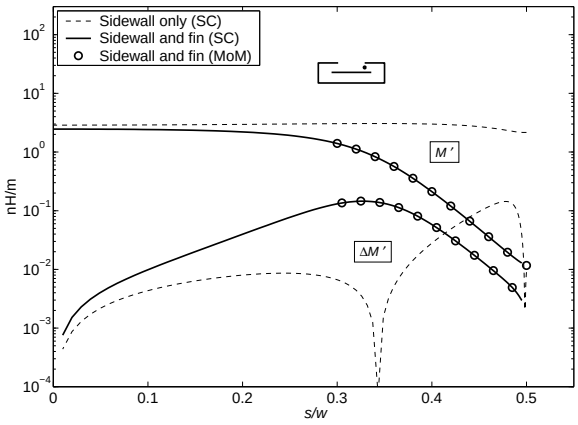

Figure 6: M' and $|\Delta M'|$ as a function of s/w for sidewall and fin of combined length $\ell = 40$ mm.

an example, in Fig. 6 we show M' and $\Delta M'$ as a function of s/w for $\ell = 40$ mm, or a sidewall of $h_{sw} = 20$ mm, with fins of the same length extending over the GP. The track is on top of the GP. For comparison, the dashed lines correspond to the data of Fig. 3 with only the sidewall of $h_{sw} = 20$ mm. Near the GP edge the fins indeed reduce $\Delta M'$. Because of the exponential variation of $M'(s)$ between the GP and fin, $|\Delta M'|$ is about $M' \times \pi \Delta s/(h_{sw} - h_{cp})$. However, $\Delta M'$ increases by more than an order of magnitude near the fin edge ($s/w = 0.35$). One observes that the range of positions where $\Delta M'$ is over 10^{-2} nH/m is extended and shifted. As a result, tracks that were not critical without the fins, may become so with them.

CONCLUSIONS

An open U-shaped cabinet panel can strongly reduce the inductive common-mode coupling of circuits on a printed circuit board, in particular when the cabinet is connected to the PCB ground plane. The reduction of M' for a single track can be accompanied by a reduction in $\Delta M'$ for a balanced pair. However, it is shown that $\Delta M'$ may even increase by an order of magnitude when the cabinet panel causes large variations in M' as a function of position. A cabinet panel extended by fins over the PCB served as an example.

The Fortran-coded numerical implementation of the Schwarz-Christoffel transformation for an unbounded doubly connected region is able to calculate very small M-couplings accurately and fast. The speed allows a systematic study of different configurations and an optimization with varying parameters.

Acknowledgments

The authors gratefully acknowledge the disinterested and effective assistance, and friendly advice of the late Prof. J. Boersma.

References

[1] F.B.M. van Horck, A.P.J. van Deursen and P.C.T. van der Laan, 'Common-mode currents generated by circuits on a PCB-measurements and transmission-line calculations,' *IEEE Trans. Electromagn. Compat.*, 43(4): 608, 2001
[2] C. Darwin, 'Some conformal mappings involving elliptic functions,' *Phyl. Mag. 41: 1, 1950*
[3] A.P.J. van Deursen, F.B.M. van Horck, M.J.A.M. van Helvoort and P.C.T. van der Laan, 'Transfer impedance of nonmagnetic conduits of various shapes', *IEEE Trans. Electromagn. Compat.* 43(1): 18, 2001
[4] T.A. Driscoll and L.N. Trefethen, *Schwarz-Christoffel Mapping*, Cambridge: Cambridge University Press, 2002
[5] A.P.J. van Deursen, 'Schwarz-Christoffel analysis of cable conduits with noncontacting cover', *El. Letters* 37(13): 816, 2001
[6] A.P.J. van Deursen and S. Kapora, 'Reduction of Inductive Common-Mode Coupling of Printed Circuit Boards by Nearby U-shaped Metal Cabinet Panel', IEEE Trans. Electromagn. Compat., (in print).
[7] H.D. Däppen, *Die Schwarz-Christoffel-Abbildung für zweifach zusammenhängende Gebiete mit Anwendungen*, PhD. thesis, ETH Zürich, 1988.
[8] P. Henrici, *Applied and Computational Complex Analysis*, Vol. 3, New York: John Wiley, 1986.
[9] C. Hu, http://www.netlib.org/toms/785 [on-line]